DOI: 10.24930/1681-9004-2023-23-6-1027-1037

Subsurface delineation of Sukadana Basalt Province based on gravity method, Lampung, Indonesia

Luhut Pardamean Siringoringo[1, 2], Benyamin Sapiie[1], Alfend Rudyawan[1], I Gusti Bagus Eddy Sucipta[1]

[1]Bandung Institute of Technology, Bandung 40132, Indonesia, e-mail: luhut_pardamean@yahoo.co.id
[2]Sumatra Institute of Technology, South Lampung 35365, Indonesia

Received 28.04.2023, accepted 14.06.2023

Research subject. The geological profile of Sukadana Basalt Province as a large basalt outcrop in the back arc of Sumatra remains to be unclear. This also concerns the geological structures and their relationship with the Sundaland regional geology. *Aim*. To reveal the type and pattern of geological structures that controlled the Sukadana Basalt Province (SBP) to the surface, the distribution of Sukadana Basalt on subsurface and its relationship with Sundaland regional tectonics. *Materials and Methods*. A reprocessed bouguer anomaly map of Tanjungkarang quadrangle 1991 was used. *Results*. We found that the main eruption was located in the center of SBP. The forward modeling data show the thickness of SBP to reach 3,200 m. There are two Northwest-Southeast striking normal faults and one fissure controlling the development of SBP. These fractures served as the primary conduit for magma to ascend from the mantle to the Earth's surface. We also found North-South striking normal faults and West-East dextral strike-slip fault that formed at Early Oligocene and indirectly supported the magma ascend to the surface. *Conclusions*. The North-South striking normal faults were correlated with the Sundaland oroclinal bending. These faults developed through the extrados zone, a large pull-apart area that caused the continental lithosphere to become thinner. Meanwhile, Quaternary-Northwest-Southeast striking fractures are correlated with the development of the Great Sumatra Fault. The formation of Northwest-Southeast striking fractures was affected by the Great Sumatra Fault movement, and the thinning of the back-arc crust affected by multi-extensional structures was implicated in the ascend of SBP's magma to the surface.

Keywords: *Sukadana Basalt, Sumatra Fault, Sundaland, Gravity, Normal fault*

Acknowledgements

We express gratitude to the Institut Teknologi Sumatera for Doctoral scholarship funding, the Geological Survey Center of Indonesia, the local government of Lampung, Sukadana society, QGIS developer, Inkscape developer, Google, and Virgian Rahmanda for his best technical contribution.

Приповерхностная характеристика базальтов провинции Сукадана на основе гравитационного метода (Лампунг, Индонезия)

Л. П. Сирингоринго[1, 2], Б. Сапийе[1], А. Рудьяван[1], И. Г. Б. Е. Сусипта[1]

[1]Бандунгский технологический институт, 40132, Бандунг, Индонезия, e-mail: luhut_pardamean@yahoo.co.id
[2]Сумматринский технологический институт, 35365, Южный Лампунг, Индонезия

Поступила в редакцию 28.04.2023, принята к печати 14.06.2023

Объект исследований. Геологический профиль базальтовой провинции Сукадана на тыловой дуге у края о-ва Суматра привлекает внимание исследователей неясным положением геологических структур и их взаимоотношением с региональной геологией Сундаленд. *Цель работы*. Выяснение типа и характера геологических структур, контролирующих базальтовую провинцию Сукодана (SBP) на поверхности, распределение базальта Сукадана в недрах и его связь с региональной тектоникой Сундаленда. *Материалы и методы*. Была проведена вторичная обработка карты аномалий Буге (1991) на территории квадрата Тан-юнгкаранг. *Результаты*. В ходе работы было обнаружено, что главное извержение располагалось в центре (SBP). Данные последующего моделирования показа-

For citation: Siringoringo L.P., Sapiie B., Rudyawan A., Sucipta I.G.B.E. (2023) Subsurface delineation of Sukadana Basalt Province based on gravity method, Lampung, Indonesia. *Lithosphere (Russia)*, **23**(6), 1027-1037. (In Russ.) https://doi.org/10.24930/1681-9004-2023-23-6-1027-1037

Для цитирования: Сирингоринго Л.П., Сапийе Б., Рудьяван А., Сусипта И.Г.Б.Е. (2023) Приповерхностная характеристика базальтов провинции Сукадана на основе гравитационного метода (Лампунг, Индонезия). *Литосфера*, **23**(6), 1027-1037. https://doi.org/10.24930/1681-9004-2023-23-6-1027-1037

ли, что мощность (SBP) достигает 3200 м. Установлено, что развитие (SBP) контролировалось двумя нормальными разломами СЗ-ЮВ простирания и одной трещинной структурой. Эти разрывы служили первичными каналами магмы, поднимающейся от мантии к земной поверхности. Был также выявлен нормальный разлом меридионального простирания и широтный правосторонний сдвиг, которые образовали ранне-олигоценовую дополнительную подвижку магмы к поверхности. *Заключение*. Нормальные меридиональные разломы коррелировали с ороклинальным изломом Сундаленда. Эти разломы развивались в пределах широкой раздвиговой площади, что способствовало утонению континентальной литосферы. Между тем, четвертичные СЗ-ЮВ трещины коррелируют с развитием Большого разлома Суматры. При его исследовании обращают на себя внимание две ключевые точки: образование СЗ-ЮВ трещин было вызвано движением Большого разлома Суматры, а утоньшение островодужной части коры происходило благодаря многочисленным структурам растяжения, которые способствовали подъему к поверхности (SBP) магмы.

Ключевые слова: *базальты Сукодна, разлом Суматра, Сундаленд, гравитация, нормальный (прямой) разлом*

Благодарности

Авторы выражают глубокую благодарность Технологическому институту Суматры за финансирование докторской стипендии, Центру геологических исследований Индонезии, местному правительству Лампунга, обществу Сукадана, разработчику QGIS, разработчику Inkscape, Google и Вирджиану Рахманде за его лучший технический вклад.

INTRODUCTION

Indonesia is part of the Sundaland Block with the highest number of active volcanoes compared to other countries in the Sundaland Block (Fig. 1a; Metcalfe, 2017). Sundaland is the continental promontory of the Eurasian plate in SE Asia (Hall and Morley, 2004). The volcanoes result from the subduction of the Australian, Indian, Pacific, and Philippine oceanic plates beneath the SE Asia (Pramumijoyo and Sebrier, 1991; Stein and Okal, 2005; Abdurrachman et al., 2018). These volcanoes are created by the accumulation of magma on the surface. The magma is produced from the partial melting process of the ocean plate at a depth range of 150–300 km (Ringwood, 1990). Oceanic plate subduction forms a convergent subduction system composing the Andaman-Sumatra-Java trench in the West and South and the Philippine Trench in the East (Li et al., 2021). In addition to producing volcanoes, this subduction also creates earthquakes, one of the largest of which occurred on December 26, 2004, Mw 9.1–9.3 (Stein and Okal, 2005).

One of the former active volcanoes, which is thought to be closely related to subduction, is Sukadana Basalt Province (SBP). SBP, also part of Sundaland, is located in the back arc of Sumatra in the Lampung Province (Fig. 1b). SBP can be similar to continental flood basalt, a short-duration eruption dominated by extrusive and intrusive rocks composed of mafic minerals (Coffin and Eldholm, 1994; Ketchum et al., 2013). This is supported by previous research on the age of SBP. Nishimura et al. (1986) stated that the age of SBP is about 0.8 Ma. Other studies show that SBP is 1.2 Ma (Soeria-Atmaja et al., 1986) and 0.46 Ma–1.15 Ma (Romeur, 1991). On this basis, SBP is considered to have a Quaternary age and experienced a short-duration eruption. This is the same age as Mount Rajabasa (Mangga et al., 1993; Hasibuan et al., 2020). In term of structures, Soeria-atmaja (1986) interpreted that the Northwest-Southeast striking fault controlled the appearance of SBP. Meanwhile, Nishimura (1986) interpreted that SBP was controlled by a Northeast-Southwest striking fracture. However, the geological structures of SBP, the distribution on the subsurface, as well as its relation to the regional tectonics are still unclear. The spreading of cinder cones in SBP can form four possible lineament patterns (Fig. 1c). These lineaments may be related to the development of geological structures (Fig. 1d).

Figure 2 illustrates the presence of a Northwest-Southeast striking pattern of SBP, which is parallel to the Great Sumatra Fault (SGF) (Fig. 1b). Moreover, the figure reveals a high degree of tectonic complexity reflected in the exposed older rocks (Mangga et al., 1993), which makes this study particularly interesting. The study aims to address the following questions: (1) What type and pattern of geological structures controlled the emergence of Sukadana Basalt to the surface?; (2) What is the subsurface distribution of Sukadana Basalt?; (3) What is the relationship between the development of geological structures and the tectonics of Sundaland region? To answer these questions, we used a gravity method, which involves the superposition of all anomalies induced by various geological sources at different depths (Nguiya et al., 2019). The separation of gravity data into its residual and regional components is crucial for the interpretation process. The answers to these questions will shed light on the structural evolution of SBP volcanism and its relation to regional tectonics. The findings from this study will enhance our understanding of the relationship between the ascend of Sukadana Basalt to the surface and the geological structure and regional tectonics of the Southeast Asian region.

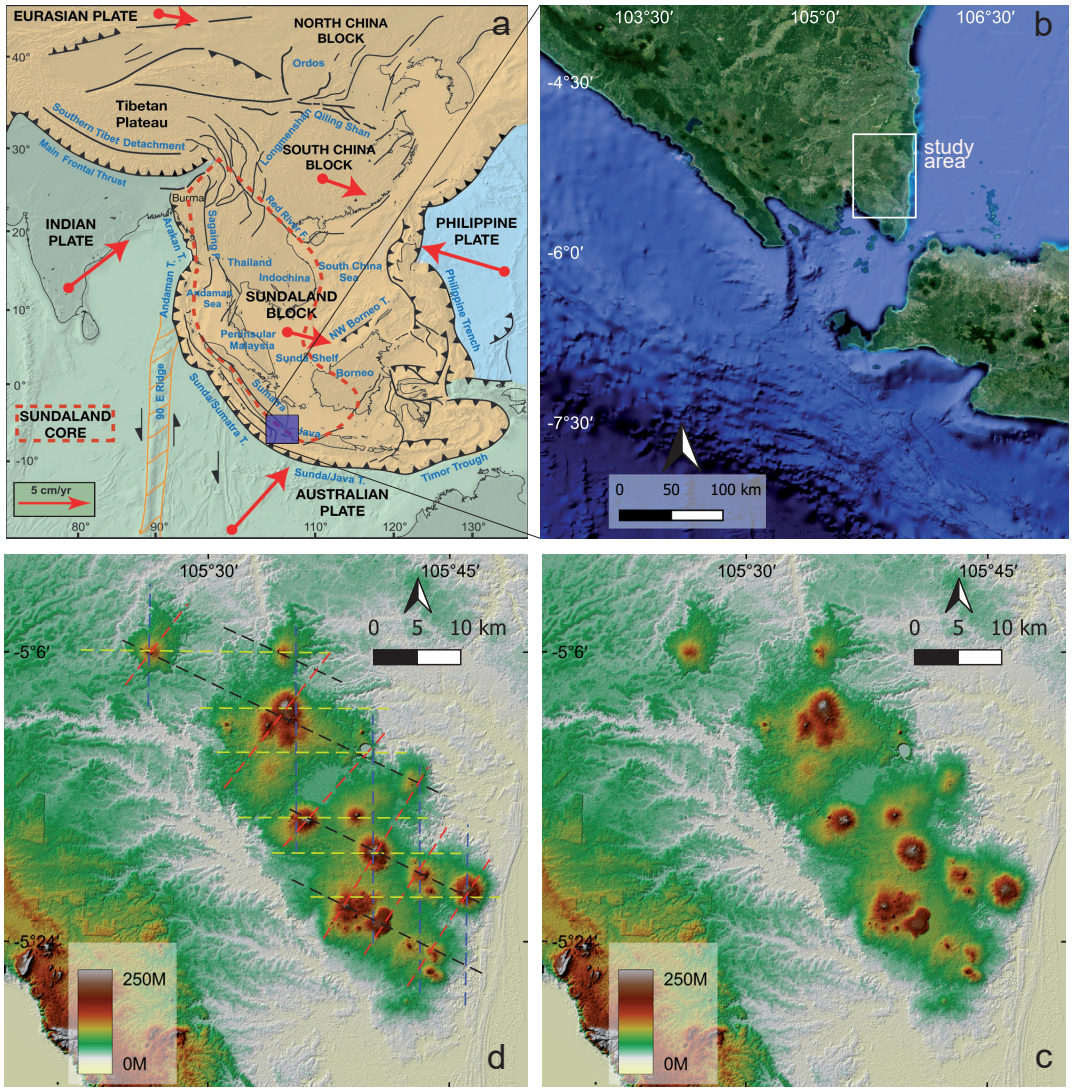

Fig. 1. (a) The tectonic region of Asia with the location of the research area within the south of Sumatra Island (blue square) (based on Metcalfe, 2017); (b) The location of Sukadana Basalt in the back arc at the tip of Sumatra Island (white line rectangle); (c) The Digital Elevation Model of Sukadana Basalt shows distribution and various sizes of cinder cones; (d) The four possible cinder cone lineament patterns of Sukadana Basalt that may be related to the development of geological structures.

Рис. 1. (a) Азиатский тектонический регион с расположением площади исследований в южной части о-ва Суматра (голубой квадрат), по (Metcalfe, 2017); (b) Размещение базальтов Сукадана в тыловой дуге у края о-ва Суматра (белый прямоугольник); (c) цифровая высотная модель базальтов Сукадана, демонстрирующая размещение и вариации размера шлаковых конусов; (d) четыре возможных линеаментных размещения шлаковых конусов базальтов Сукадана, возможно связанных с развитием геологических структур.

MATERIALS AND METHODS

The gravity method is a geophysical method that utilizes earth gravity to image subsurface rocks based on its density diversity (Wardhana et al., 2014). This method is commonly used as an early hydrocarbon and mineral exploration survey (Setiadi et al., 2019). In this study, the gravity method was used to determine subsurface geology conditions, including the type of fault and its orientation, lithology, and its distribution.

The gravity data used in this study was sourced from the Bouguer Anomaly map of the Tanjungkarang quadrangle 1991 from the Indonesia Geological Survey Center. The data was further processed with terrain corrections. The gravimeter used for measurement was La Coste & Romberg model G (Seigel, 1995). The data was acquired by following public roads and accessible locations, with intervals ranging from 2 km to 5 km. A total of 56 retrieval points were used in this study, covering the Sukadana Basalt and its surrounding areas.

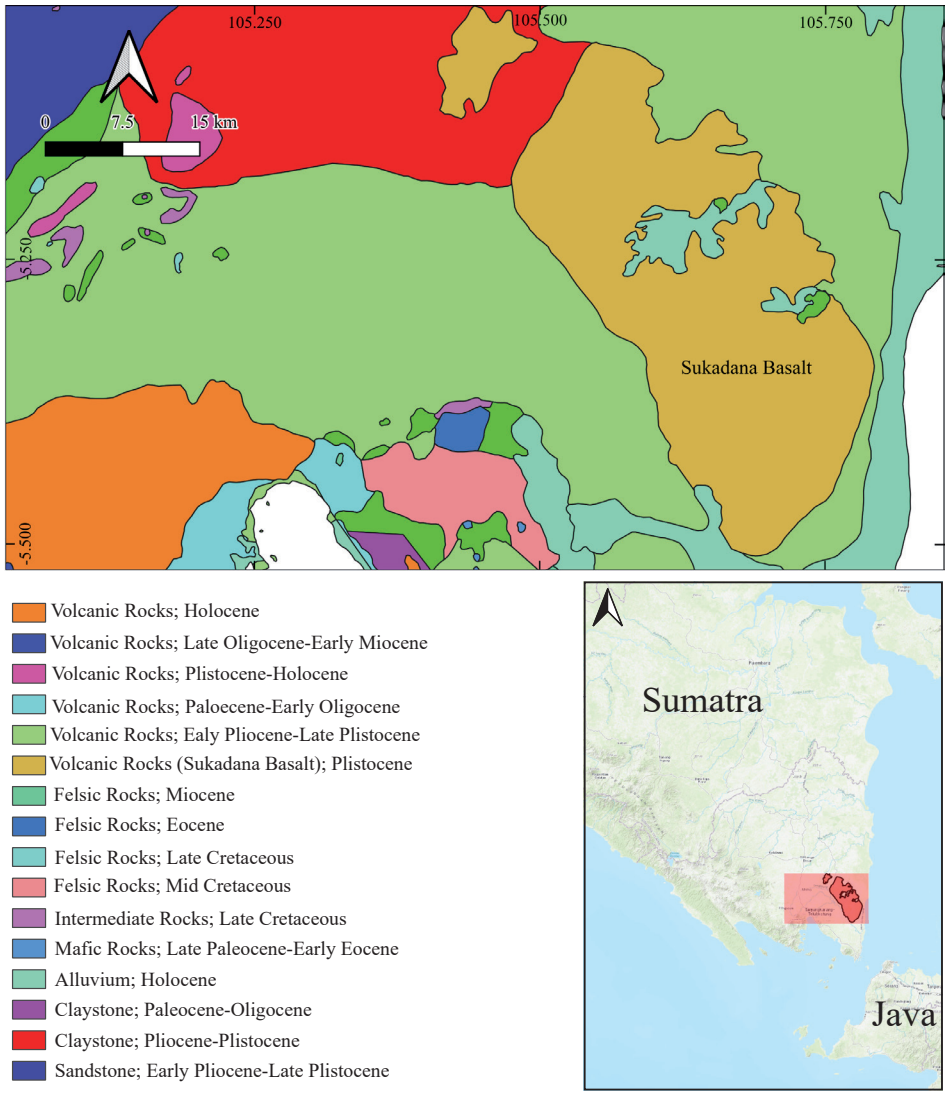

Fig. 2. The Basalt Sukadana and its surrounding geology according to the Tanjungkarang quadrangle regional geology (Mangga et al., 1993).

Рис. 2. Базальты Сукадана и прилегающие породы в соответствии с прилегающей Тан-юнгкаранг региональной геологией (Mangga et al., 1993).

The software that was used for processing the gravity data was Oasis Montaj 8.3.3 (Developer, 2019). We separated the regional and residual anomalies from the Bouguer anomaly by applying a moving average filter approach to obtain more accurate information. This separation is an important step in interpretation (Nguiya et al., 2019), helping in identifying anomaly patterns that can describe the sub-surface structures and lithology from the deepest to the shallowest depth (Siringoringo et al., 2021).

A Digital Elevation Model (DEM), used as a base map or topographic map in this study, was downloaded from tanahair.indonesia.go.id/demnas. DEM, or DEMNAS (DEM Nasional). This is an integration of data from IFSAR, TERRASAR-X and ALOS PALSAR. DEMNAS has a spatial resolution of 8 m (Julzarika and Harintaka, 2019). The entire maps are processed using Quantum Geographic Information System (QGIS) 3.22.5 and the Coordinate Reference System (CRS) WGS 84 (Contributor, 2022). Through this DEM, we determined the cinder cones or basalt cone boundary based on the assumption that the slope level of the cinder cones reflects the degree of thickness of the cinder cones deposit. This means that the nearly plain slope reflects a thinner thickness of lava. The basalt cones distribution would be overlaid to the all maps to obtain better interpretation. All images other than maps were processed using the Inkscape software (Inkscape's Contributors, 2022).

RESULTS AND DISCUSSION

Gravity anomaly interpretations

The residual anomaly map over SBP shows the gravity anomaly region variation from –0.7 to 0.5 mGal. This is associated with density contrasts due to different lithologies (Fig. 3). Lithology interpretation is based on the assumption that low-density rocks indicate sedimentary rocks, while high-density rocks are igneous or metamorphic rocks (Evariste et al., 2014). The low gravity also reflects high-porosity sediments or volcanic tuffs (Lichoro et al., 2019). The residual anomaly map classifies the basement basin, quarterly sedimentary rocks, and volcanic deposits in terms of their specific features. The comparison with the geology map (Fig. 2), a low gravity anomaly with an amplitude of about <–0.2 mGal (blue) agrees well with Quarterly claystone, tuff and thin lava deposit of SBP. The moderate gravity anomaly (green) with an amplitude of about –0.2–0.0 mGal is compatible with the thin lava deposit of SBP. High gravity (orange-purple) with an amplitude of about >0.1 mGal is associated with a thick lava deposit of SBP. This high gravity shows West-East, North-East, and Northwest-Southeast trending. The residual map also explains that the small part of SBP in the North is not basalt but rather claystone. The high gravity (>0.2 mGal) in SBP means the eruption center of SBP.

The patterns or lateral structural trends of residual anomalies are determined using a moving average filter. This is the aim of qualitative gravity interpretation (Setiadi, 2020). Integration of qualitative gravity interpretations reveals structural lineaments (Fig. 3), which might correspond to the basement boundaries controlled by faults. The lineaments show North-South, Northwest-Southeast, and West-East trending. The map shows a sharp anomaly between high gravity and low gravity, which we interpret as a fault zone. Additionally, the presence of basalt on the earth's surface is closely related to the mechanism of normal fault formation (Faccenna et al., 2010; De Souza et al., 2013; Shahraki, 2013; Wang et al., 2015; Ayalew et al., 2018; Yan et al., 2018; Zi et al., 2019). This is because raising magma from the mantle to the earth's surface requires an extensional tectonic mechanism. Therefore, in this study, we interpret those lineaments as normal faults that control the appearance and pattern of SBP on the surface.

In addition to the residual anomaly map, the regional anomaly map over SBP shows the variations of gravity anomaly from 47 to 80 mGal (Fig. 4). The Figure 4 shows the low-gravity anomaly with an amplitude of about <63 mGal (blue), the moderate-gravity anomaly (green) with an amplitude of about 63–68 mGal, whereas high gravity (orange-purple) with an amplitude of about >69 mGal. The high gravity shows West-East and Northwest-Southeast trending. The high gravity (>75 mGal) in SBP interpreted as the main eruption center of SBP. The lineaments also consist of North-South, Northwest-Southeast, and West-East trending.

Figure 5 shows the interpretation of basin depth from a radially averaged power spectrum analysis. Slope S1 shows the signal source in the basement from more than 1000 m depth. Slope S2 shows a signal source at a depth less than 1000 m. Slope S3 shows the processes of data acquisition. The graphic reveals gravity signals from shallow sources or disrupted surface noise from data acquisition processes (Kanthiya et al., 2019).

The Complete Bouguer Anomaly (CBA) map of SBP shows variations in gravity anomaly ranging from 47 to 80 mGal (Fig. 6). Low-gravity anomalies (<62 mGal) are represented by blue, while moderate-gravity anomalies (62–69 mGal) are represented by green. High-gravity anomalies (70–80 mGal) trend in a West-East and Northwest-Southeast direction, indicating the main eruption center of SBP. Generally, residual, regional, and CBA density patterns exhibit the same lineament patterns: North-South, West-East, and Northwest-Southeast, which are correlated with the development of structural geology. The distribution of basalt cones on the surface is parallel to the Northwest-Southeast striking fractures. Furthermore, the emergence of SBP on the surface was directly controlled by two Northwest-Southeast striking normal faults and one fissure (Fig. 6).

Forward Models and Tectonics Significance

The subsurface geometry of SBP was generated by forward models from gravity data, revealing a maximum basin depth of around 3,200 m, two normal faults, and one fissure. The fissure crossed the dextral strike-slip fault (Fig. 7). According to the Tanjungkarang regional geology map and surface geology constraints, the basement of SBP is Gunungkasih schists, bounded by Lampung Formation (Qtl) in its surroundings.

The North-South striking pattern is interpreted as normal faults. These faults are part of the Sumatra oroclinal bending. The Sumatra oroclinal bending was closely formed in relation to the India collision with Eurasia (Figs. 8a and 8b). These normal faults are associated with the extrados zone, a large pull-apart area resulting from parallel strike-slip fault movement from the Sundaland orocline (Hutchison 2010; Fig. 8a and 8b). An orocline is a thrust belt or orogen that is curved in map view due to bending or buckling about a vertical axis of rotation (Johnston et al., 2013). The extrados zone results in the continental lithosphere thickness to become thinner, which is one of the controllers of magma appearance on the surface (Fan et al., 2021; Zhang et al., 2022). Bora et al. (2016) stated that the thickness of the Sumatran crust ranges within 27–35 km, which is relatively thin according to Curie and Hyndman (2006). Furthermore, the extrados zone indirectly facilitates the magma ascend towards

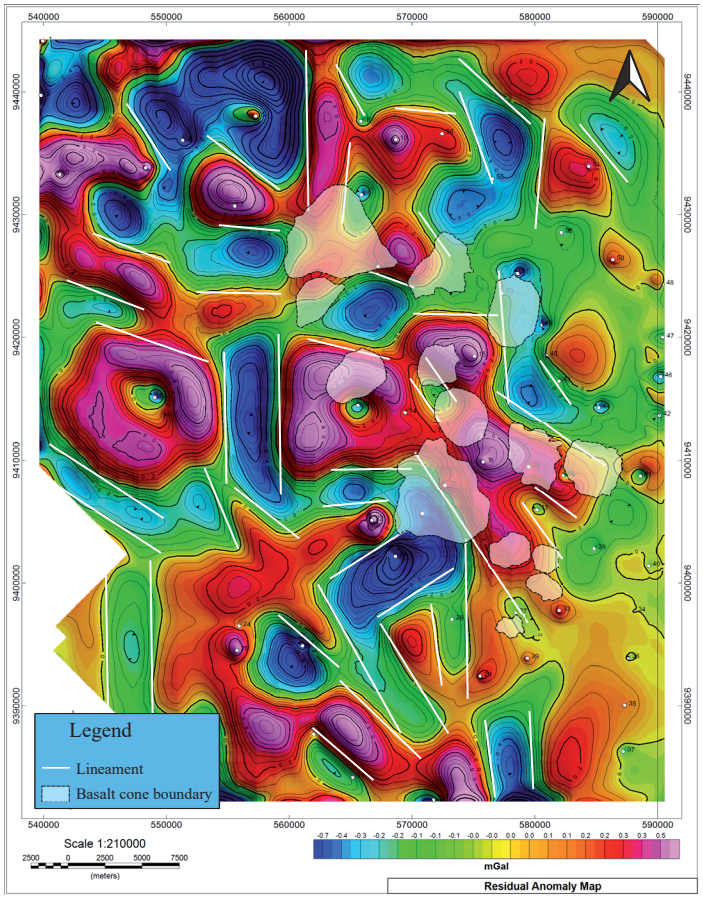

Fig. 3. The residual anomaly map of SBP. There are three lineaments trending: North-South, West-East, and Northwest-Southeast.

Рис. 3. Карта остаточных аномалий SBP. Наблюдаются три линеаментных тренда: С-Ю, З-В и СЗ-ЮВ.

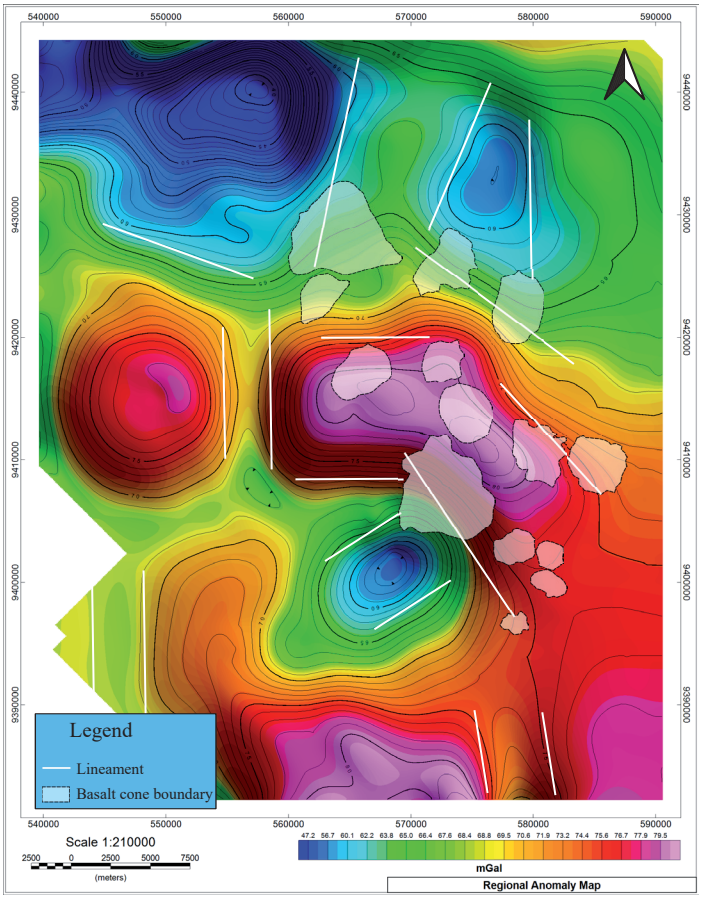

Fig. 4. The regional anomaly map of SBP with lineaments interpretation.

Рис. 4. Региональная карта аномалий SBP с линеаментной интерпретацией.

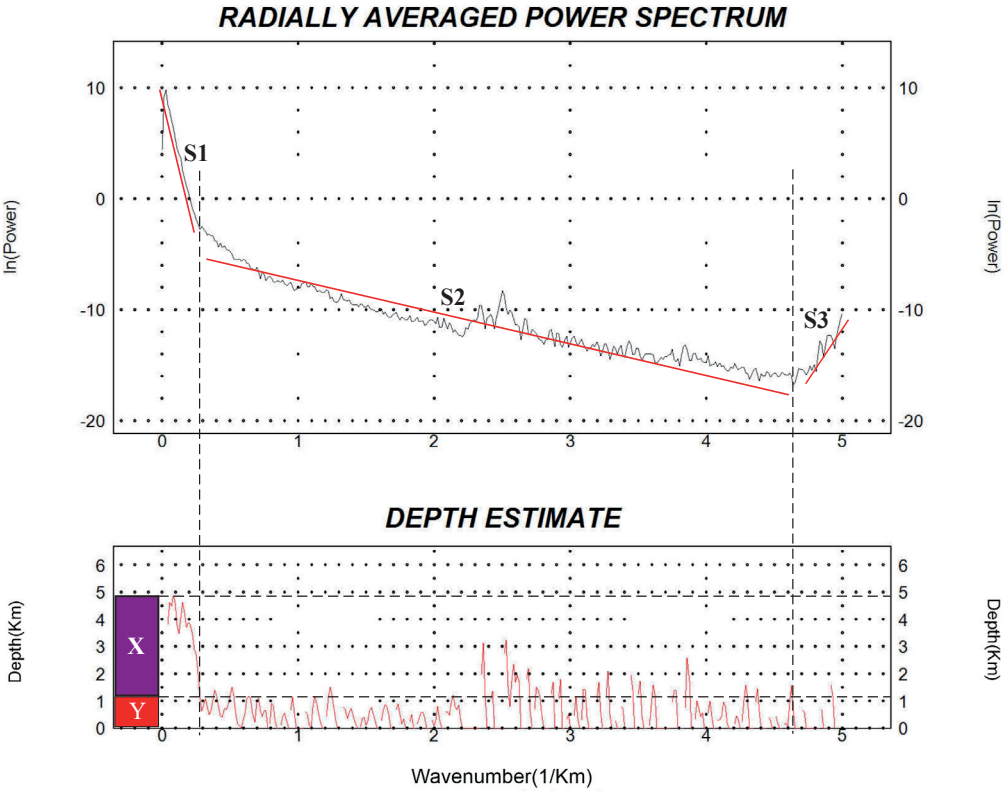

Fig. 5. The estimated average depth of SBP (Y) and basement basin (X) and three slopes show gravity sources: slope S1 (deep), slope S2 (shallow), and slope S3 (near-surface).

Рис. 5. Приблизительная средняя оценка глубины SBP (Y) и основания бассейна (X) и три наклона, показывающие источники деформаций: наклон S1 (глубокий), наклон S2 (мелкий) и наклон S3 (близповерхностный).

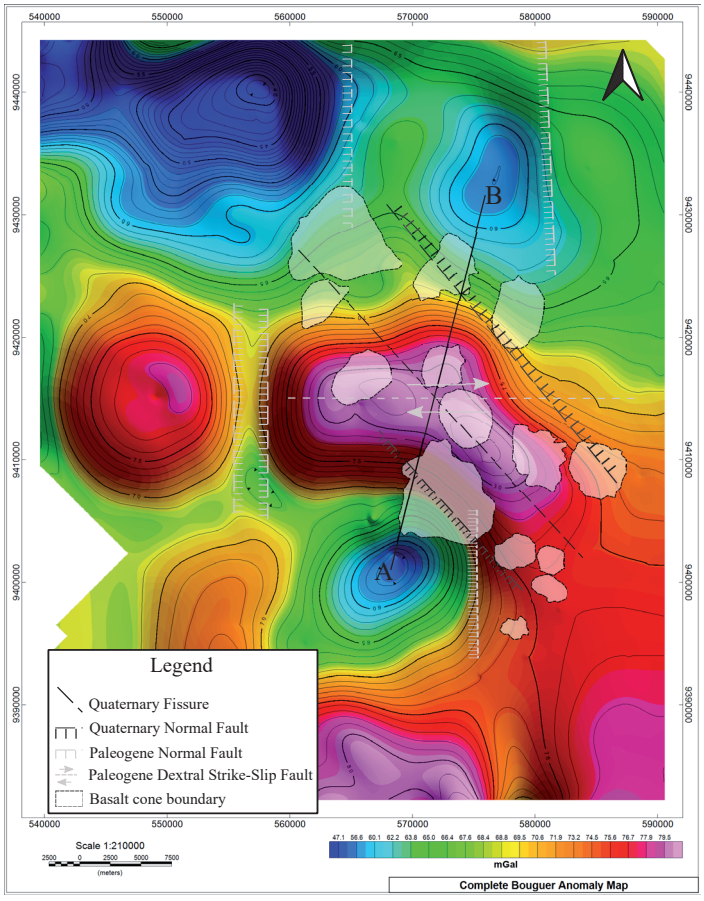

Fig. 6. The Complete Bouguer Anomaly map of SBP which is overlaid by basalt cones boundary with fault interpretation. The development of basalt cones on the surface resulted from normal faults and fissure mechanism. The subsurface model from section A-B within Fig. 7.

Рис. 6. Завершенная карта аномалий Буге SBP, перекрытая границей базальтовых конусов с ошибочной интерпретацией. Распространение базальтовых конусов по поверхности вызвано сочетанием нормальных разломов и трещинного механизма. Приповерхностная модель на разрезе АВ – см. рис. 7.

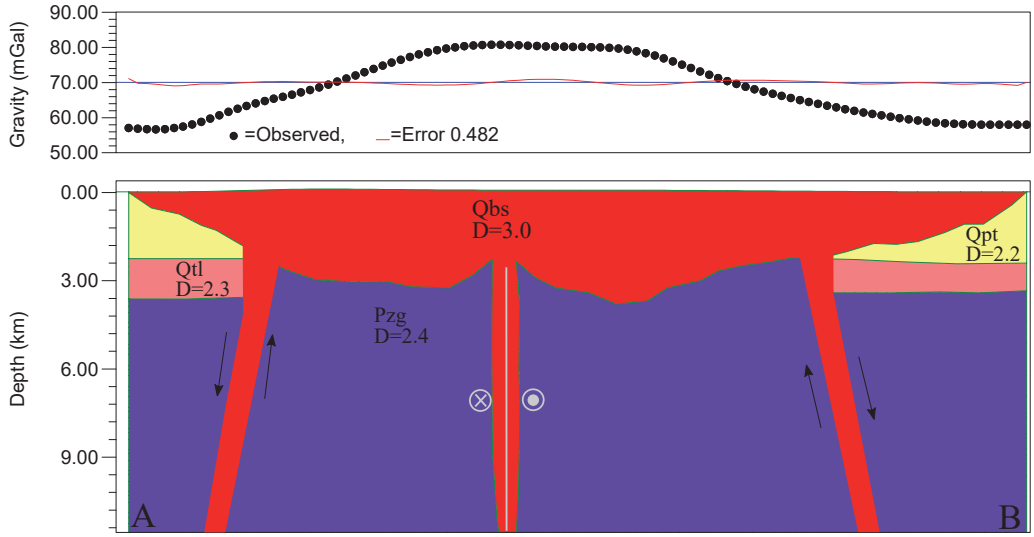

Fig. 7. The profiles of forward modelling show that the thickness of SBP reaches 3,200 m. Two normal faults and one fissure have been identified. These fractures controlled the appearance of SBP's lava at the surface. In addition, there is a Paleogene dextral strike-slip fault was identified.

Рис. 7. Профили предварительного моделирования свидетельствуют о том, что мощность SBP достигала 3200 м. Были идентифицированы два нормальных разлома и одна трещинная зона. Такие трещины контролировали появление лав SBP на поверхности. К тому же был обнаружен правосторонний сдвиг.

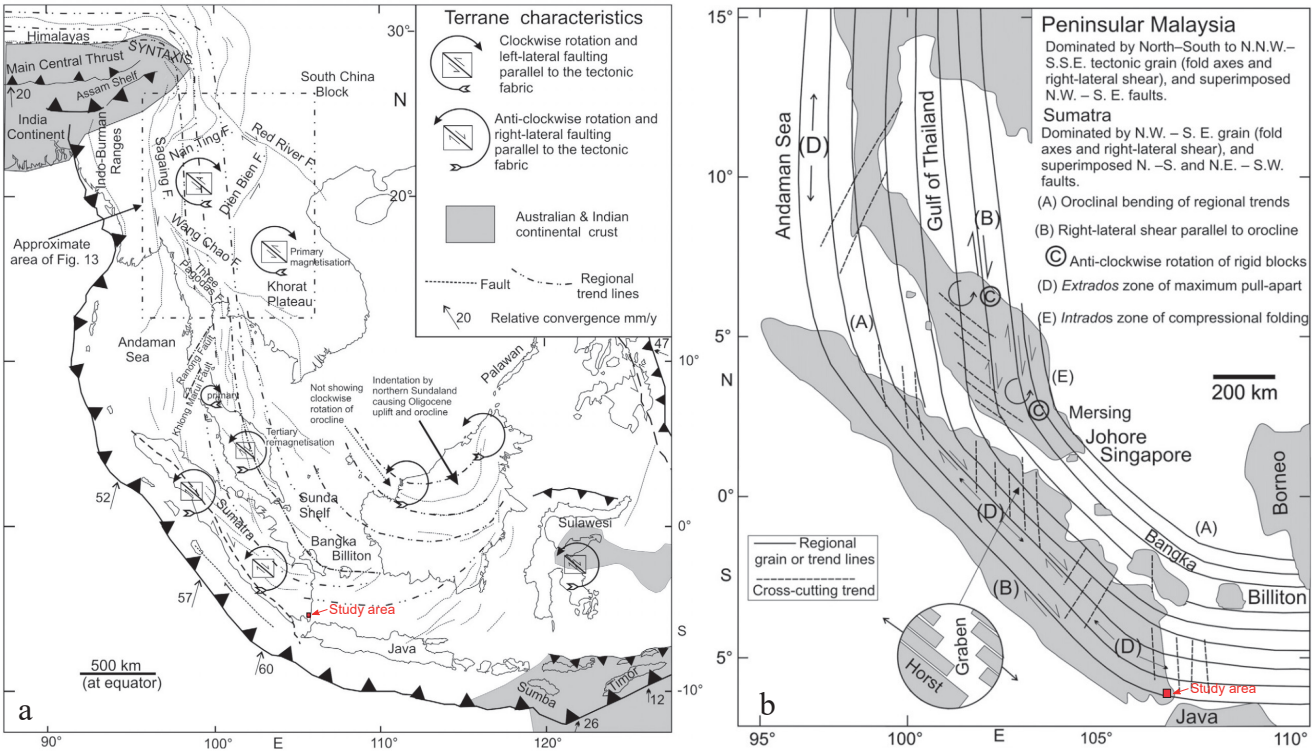

Fig. 8. (a) The oroclinal bending in South-East Asia. The India-Eurasia collision was resulting left and right lateral faulting in South-East Asia. (b) The movement of the right-lateral strike-slip faulting made extrados zone where the SBP is located. The pictures from Hutchison (2010). The red square shows the SBP location.

Рис. 8. (a) Ороклинный изгиб в Юго-Восточной Азии. Индо-Евразийская коллизия вызвала левые и правые латеральные дислокации в Юго-Восточной Азии. (b) Движение по правостороннему сдвигу привело к образованию зоны SBP (Hutchison, 2010). Красное поле указывает на размещение SBP.

the surface. There is a close relationship between pull-apart basins and volcano-magmatic activity (Girard and van Wyk de Vries, 2005; Susilohadi et al., 2009). However, the origin of the bending is still an enigma (Hutchison, 2010). The North-South striking normal faults in the SBP were formed in the Early Oligocene. This is based on a comparison to the Sunda-Asri Basin forming mechanism, which began in the Early Oligocene (Doust and Noble, 2008). The SBP's North-South striking normal fault is the same trend and parallel with the Sunda-Asri Basin's North-South striking normal fault. The Sunda-Asri Basin is located on the east side of the SBP.

The West-East striking pattern is interpreted as a consequence of the dextral strike-slip fault movement that might be related to the Sundaland orocline (Fig. 8b). This fault is located in the middle of the SBP. The age of this structure is Early Oligocene, the same age as the North-South striking normal fault. This dextral strike-slip fault indirectly controlled the distribution of the SBP on the West-East trend.

The Northwest-Southeast striking pattern is interpreted as normal faults. In addition, there is one fissure in the middle of SBP, which has the same trending as the Northwest-Southeast normal faults. The Northwest-Southeast striking normal fault and fissure are interpreted as the main structures that have emerged the SBP to the surface. These structures are the same age as the Panjang fault, which is Quaternary age. There are three pieces of evidence supporting this interpretation: firstly, the age of the SBP is also Quaternary; secondly, the location of the fault is close to the Panjang fault (which crosses Mount Rajabasa, as shown in Fig. 9); and thirdly, the trending of the faults is parallel with the Panjang fault. Pramumijoyo and Sebrier (1991) stated that the Panjang Fault was caused by the opening of the western part of Sunda Strait, and the development of structures in the Sunda Strait is

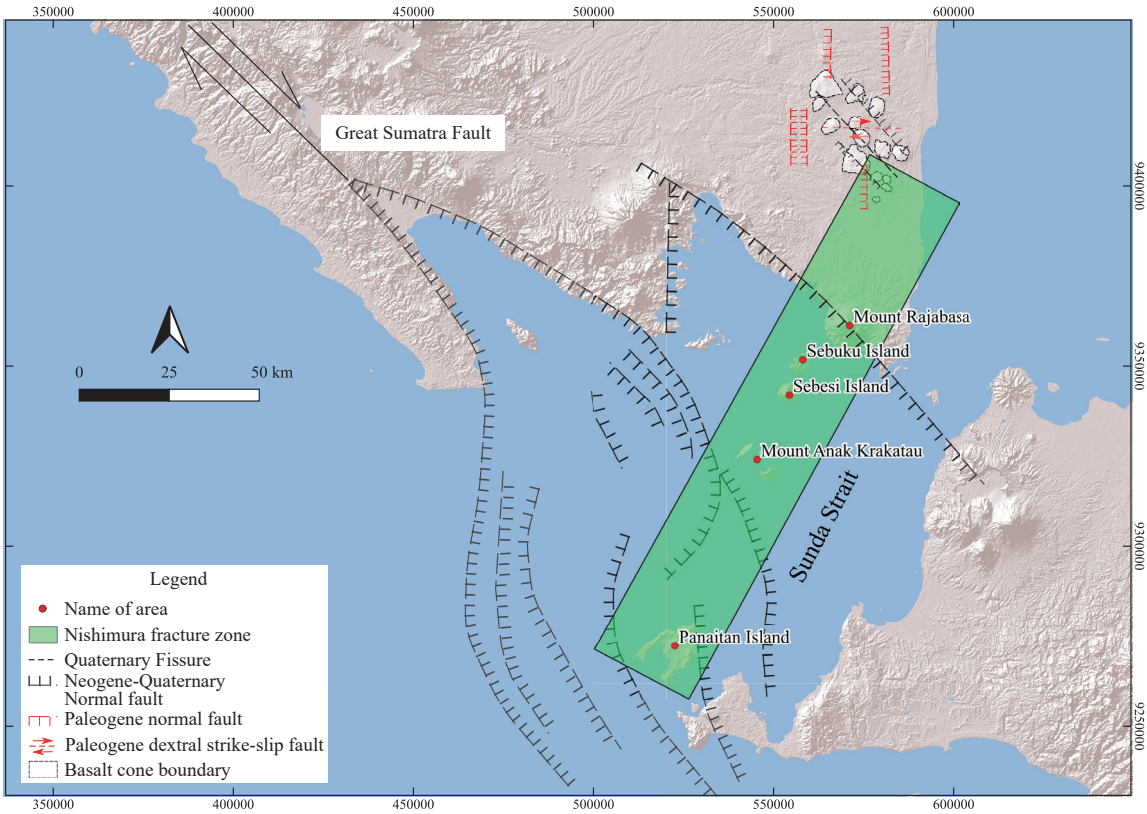

Fig. 9. The correlation of structures at SBP with regional fault trending at Sunda Strait. The Northwest-Southeast fractures at SBP are parallel with The Great Sumatra Fault, indicating that the structures at SBP still correlate with the development of the Great Sumatra Fault. The normal fault interpretation at Mount Rajabasa is based on (Pramumijoyo, Sebrier, 1991), at the Western part of Sunda Strait on (Susilohadi et al., 2009) and the green shading zone on (Nishimura et al., 1986).

Рис. 9. Корреляция структур SBP с региональным трендом вблизи пролива Сунда. СЗ-ЮВ разломы SBP параллельны Большому разлому Суматры, это свидетельствует о том, что структуры SBP еще коррелируют с развитием Большого разлома Суматры. Прямая интерпретация разлом Горы Раябаса, по (Pramumijoyo, Sebrier, 1991), в западной части пролива Сунда, по (Susilohadi et al., 2009) и зеленой тенистой зоны, по (Nishimura et al., 1986).

still correlated with the development of the Sumatra fault tectonic (Susilohadi et al., 2009). Furthermore, the development of the Northwest-Southeast striking normal fault and fissure at the SBP was caused by the Sumatra fault tectonic.

CONCLUSIONS

We conclude that the geological structures that controlled the SBP development were two Northwest-Southeast striking normal faults and one fissure. These fractures acted as the main conduits for magma to ascend from the mantle to the surface. The forward modeling data shows that the thickness of SBP reaches 3,200 m at the center. The North-South striking normal fault and West-East striking dextral strike-slip fault, which formed in the Early Oligocene, indirectly supported the magma ascent to the surface. The development of the North-South striking normal fault through the extrados zone, a large pull-apart area, resulted in the continental lithosphere thickness becoming thinner.

In relation to the Sundaland regional geology, the North-South and West-East striking faults are correlated with the Sundaland oroclinal bending. This bending is indirectly affected by the India-Eurasia collision. One of the impacts of this collision was the development of multiple strike-slip faults in Southeast Asia. This resulted in the formation of an extrados zone where SBP is located. The Quaternary Northwest-Southeast striking fractures are correlated with the development of the Great Sumatra Fault. There are two key points from this study. First, the formation of Northwest-Southeast striking fractures was affected by the Great Sumatra Fault movement. Second, the thinning of the back-arc crust affected by multi-extensional structures was implicated in the ascent of SBP's magma to the surface.

REFERENCES

Abdurrachman M., Widiyantoro S., Priadi B., Ismail T. (2018) Geochemistry and structure of krakatoa volcano in the Sunda Strait, Indonesia. *Geosci.*, **8**, 1-10. https://doi.org/10.3390/geosciences8040111

Ayalew D., Jung S., Romer R.L., Garbe-Schönberg D. (2018) Trace element systematics and Nd, Sr and Pb isotopes of Pliocene flood basalt magmas (Ethiopian rift): A case for Afar plume-lithosphere interaction. *Chem. Geol.*, **493**, 172-188. https://doi.org/10.1016/j.chemgeo.2018.05.037

Bora D.K., Borah K., Goyal A. (2016) Crustal shear-wave velocity structure beneath Sumatra from receiver function modeling. *J. Asian Earth Sci.*, **121**, 127-138. https://doi.org/10.1016/j.jseaes.2016.03.007

Coffin M., Eldholm O. (1994) Large igneous provinces: Crustal structure, dimensions, and external consequences. *Revs. Geophys.*, **32**, 1-36.

Contributor Q. (2022) QGIS.org.

Curie C.A., Hyndman R.D. (2006) The thermal structure of subduction zone back arcs. *J. Geophys. Res. Solid Earth*, **111**, 1-22. https://doi.org/10.1029/2005JB004024

De Souza Z.S., Vasconcelos P.M., Knesel K.M., da Silveira Dias L.G., Roesner E.H., Cordeiro de Farias P.R., de Morais Neto J.M. (2013) The tectonic evolution of Cenozoic extensional basins, northeast Brazil: Geochronological constraints from continental basalt $^{40}Ar/^{39}Ar$ ages. *J. South Am. Earth Sci.*, **48**, 159-172. https://doi.org/10.1016/j.jsames.2013.09.008

Developer O.M. (2019) Geosoft Oasis Montaj Data Processing and Analysis Systems for Earth Science Applications.

Doust H., Noble R. (2008) Petroleum systems of Indonesia. *Mar. Pet. Geol.*, **25**, 103-129.

Evariste N.H., Genyou L., Tabod T.C., Joseph K., Severin N., Alain T., Xiaoping K.E. (2014) Crustal structure beneath Cameroon from EGM2008. *Geod. Geodyn.*, **5**, 1-10. https://doi.org/10.3724/sp.j.1246.2014.01001

Faccenna C., Becker T.W., Lallemand S., Lagabrielle Y., Funiciello F., Piromallo C. (2010) Subduction-triggered magmatic pulses: A new class of plumes? *Earth Planet. Sci. Lett.*, **299**, 54-68. https://doi.org/10.1016/j.epsl.2010.08.012

Fan X., Chen Q.F., Ai Y., Chen L., Jiang M., Wu Q., Guo Z. (2021) Quaternary sodic and potassic intraplate volcanism in northeast China controlled by the underlying heterogeneous lithospheric structures. *Geology*, **49**, 1260-1264. https://doi.org/10.1130/G48932.1

Girard G., van Wyk de Vries B. (2005) The Managua Graben and Las Sierras-Masaya volcanic complex (Nicaragua); pull-apart localization by an intrusive complex: results from analogue modeling. *J. Volcanol. Geotherm. Res.*, **144**, 37-57. https://doi.org/10.1016/j.jvolgeores.2004.11.016

Hall R., Morley C.K. (2004) Sundaland basins, in: Geophysical Monograph Series. American Geophysical Union, 55-85. https://doi.org/10.1029/149GM04

Hasibuan R.F., Ohba T., Abdurrachman M., Hoshide T. (2020) Temporal Variations of Petrological Characteristics of Tangkil and Rajabasa Volcanic Rocks, Indonesia. Indones. *J. Geosci.*, **7**, 135-159. https://doi.org/10.17014/ijog.7.2.135-159

Hutchison C.S. (2010) Oroclines and paleomagnetism in Borneo and South-East Asia. *Tectonophysics*, **496**, 53-67. https://doi.org/10.1016/j.tecto.2010.10.008

Inkscape's Contributors (2022) Inkscape.

Johnston S.T., Weil A.B., Gutierrez-Alonso G. (2013) Oroclines: Thick and thin. *Geol. Soc. Am. Bull.*, **125**, 643-663. https://doi.org/10.1130/B30765.1

Julzarika A., Harintaka (2019) Indonesian DEMNAS: DSM or DTM?, in: AGERS 2019 - 2nd IEEE Asia-Pacific Conference on Geoscience, Electronics and Remote Sensing Technology: Understanding and Forecasting the Dynamics of Land, Ocean and Maritime, Proceeding. IEEE, 31-36. https://doi.org/10.1109/AGERS48446.2019.9034351

Kanthiya S., Mangkhemthong N., Morley C.K. (2019) Structural interpretation of Mae Suai Basin, Chiang Rai Province, based on gravity data analysis and modelling. *Heliyon*, **5**, e01232. https://doi.org/10.1016/j.heliyon.2019.e01232

Ketchum K.Y., Heaman L.M., Bennett G., Hughes D.J. (2013) Age, petrogenesis and tectonic setting of the Thessalon volcanic rocks, Huronian Supergroup, Canada. *Precambrian Res.*, **233**, 144-172. https://doi.org/10.1016/j.precamres.2013.04.009

Li J., Ding W., Lin J., Xu Y., Kong F., Li S., Huang X., Zhou Z. (2021) Dynamic processes of the curved subduction system in Southeast Asia: A review and future perspective. *Earth-Science Rev.*, **217**, 103647. https://doi.org/10.1016/j.earscirev.2021.103647

Lichoro C.M., Árnason K., Cumming W. (2019) Joint interpretation of gravity and resistivity data from the Northern Kenya volcanic rift zone: Structural and geothermal significance. *Geothermics*, **77**, 139-150. https://doi.org/10.1016/j.geothermics.2018.09.006

Mangga S.A., Amirudin T., Suwarti S., Gafoer dan Sidarto. (1993) Peta Geologi Lembar Tanjungkarang, Sumatra, Bandung: Pusat Penelitian dan Pengembangan Geologi.

Metcalfe I. (2017) Tectonic evolution of Sundaland. *Bull. Geol. Soc. Malaysia*, **63**, 27-60. https://doi.org/10.7186/bgsm63201702

Nguiya S., Mouzong Pemi M., Tokam A.P., Ngatchou Heutchi É., Lemotio W. (2019) Crustal structure beneath the Mount Cameroon region derived from recent gravity measurements. *Comptes Rendus - Geosci.*, **351**, 430-440. https://doi.org/10.1016/j.crte.2019.05.001

Nishimura S., Nishida J., Yokoyama T., Hehuwat F. (1986) Neo-tectonics of the Strait of Sunda, Indonesia. *J. Southeast Asian Earth Sci.*, **1**, 81-91. https://doi.org/10.1016/0743-9547(86)90023-1

Pramumijoyo S., Sebrier M. (1991) Neogene and quaternary fault kinematics around the Sunda Strait area, Indonesia. *J. Southeast Asian Earth Sci.*, **6**, 137-145. https://doi.org/10.1016/0743-9547(91)90106-8

Ringwood A. (1990) Petrogenesis of intraplate magmas and structure of the upper mantle. *Chem. Geol.*, **82**, 187-207.

Romeur M. (1991) Series magmatiques arc et arriere-arc de la sonde: nature des sources impliquees (elements en trace et isotopes Sr-Nd-Pb). These de Doctorat, Universite de Bretagne Occidentale, Brest.

Seigel H. (1995) A guide to high precision land gravimeter surveys. Ontario, Canada, 132 p.

Setiadi I. (2020) Konfigurasi Batuan Dasar dan Delineasi Sub Cekungan Banyumas Berdasarkan Analisis Data Gayaberat. *J. Geol. dan Sumberd. Miner.*, **2245**, 070034.

Setiadi I., Setyanta B., Nainggolan T.B., Widodo J. (2019) Delineation of Sedimentary Subbasin and Subsurface Interpretation East Java Basin in the Madura Strait and Surrounding Area Based on Gravity Data Analysis. *Bull. Mar. Geol.*, **34**, 1-16. https://doi.org/10.32693/bomg.34.1.2019.621

Shahraki M. (2013) Dynamics of mantle circulation and convection : The signatures in the satellite derived gravity fields. Johann Wolfgang Goethe University.

Siringoringo L.P., Paembonan A.Y., Rahmanda V. (2021) Fault Reassessment in Way Huwi Area , South Lampung using Gravity Method Fault Reassessment in Way Huwi Area. *J. Geofis.*, **19**, 36-40.

Soeria-Atmaja R., Maury R.., Bougault H., Joron J., Bellon H., Hasanunddin D. (1986) Présence de tholeiites d'arrière- arc Quatenariés en Indonésie: Les basaltes de Sukadana (Sud de Sumatra), in: Réunion Des Sciences de La Terre. Clermont- Ferrand.

Stein S., Okal E.A. (2005) Speed and size of the Sumatra earthquake. *Nature*, **434**, 581-582. https://doi.org/10.1038/434581a

Susilohadi S., Gaedicke C., Djajadihardja Y. (2009) Structures and sedimentary deposition in the Sunda Strait, Indonesia. *Tectonophysics*, **467**, 55-71. https://doi.org/10.1016/j.tecto.2008.12.015

Wang Y., Santosh M., Luo Z., Hao J. (2015) Large igneous provinces linked to supercontinent assembly. *J. Geodyn.*, **85**, 1-10. https://doi.org/10.1016/j.jog.2014.12.001

Wardhana D.D., Harjono H., Sudaryanto S. (2014) Struktur Bawah Permukaan Kota Semarang Berdasarkan Data Gayaberat. *J. Ris. Geol. dan Pertamb.*, **24**, 53. https://doi.org/10.14203/risetgeotam2014.v24.81

Yan Q., Shi X., Metcalfe I., Liu S., Xu T., Kornkanitnan N., Sirichaiseth T., Yuan L., Zhang Y., Zhang H. (2018) Hainan mantle plume produced late Cenozoic basaltic rocks in Thailand, Southeast Asia. *Sci. Rep.*, **8**(2640). https://doi.org/10.1038/s41598-018-20712-7

Zhang A., Guo Z., Afonso J.C., Handley H., Dai H., Yang Y., Chen Y.J. (2022) Lithosphere–asthenosphere interactions beneath northeast China and the origin of its intraplate volcanism. *Geology*, **50**, 210-215. https://doi.org/10.1130/G49375.1

Zi J.W., Haines P.W., Wang X.C., Jourdan F., Rasmussen B., Halverson G.P., Sheppard S., Li C.F. (2019) Pyroxene $^{40}Ar/^{39}Ar$ Dating of Basalt and Applications to Large Igneous Provinces and Precambrian Stratigraphic Correlations. *J. Geophys. Res. Solid Earth*, **124**, 8313-8330. https://doi.org/10.1029/2019JB017713